

Aerodynamic and performance analysis of an Axial flow compressor

G. Ayadju¹ and A.I. Obanor²

¹Department of Mechanical Engineering, Delta State Polytechnic, Otefe-Oghara, Delta State, Nigeria.

²Department of Mechanical Engineering, University of Benin, Benin City, Edo State, Nigeria.

Corresponding Author's E-mail: aggordonp@yahoo.co.uk

Abstract

This study intends to determine performance and aerodynamic details on the GE Frame 9E compressor unit. The objectives are to model the axial compressor performance, flow behaviour and degree of reaction distribution with Simulink. A Simulink model of GE Frame 9E compressor was used; design parameters were applied to the model; performance simulation and analysis were carried out. Results showed diffusion factor, flow, temperature, pressure coefficients and stage efficiency of 0.36 to 0.4, 0.61, 0.33, 0.3, and 0.92 respectively, and degree of reaction was between 0.67 and 0.55. At pitch-chord ratio of 0.4, diffusion factor was 0.38 at last stage. At a rotor inlet flow angle of 15°, degree of reaction and diffusion factor were from 0.4 to 0.69 and 0.46 to 0.37 accordingly as engine speed increased from 40rps to 60rps. GE Frame 9E compressor maintained high stage efficiency, and flow, temperature, pressure coefficients and diffusion factor were satisfactory. Diffusion factor decreased with reduced pitch-chord ratio, but at higher inlet flow angles diffusion factor was increased and degree of reaction was reduced, and vice versa at higher engine speed. This study has brought to the fore the performance details, the distribution of the diffusion factor and degree of reaction of a GE Frame 9E axial flow compressor, and the influence of engine speed and rotor inlet flow angle on them.

Keywords: Axial Flow Compressor, Aerodynamic and Performance Analysis, Diffusion Factor, GE Frame 9E Compressor.

1. Introduction

An axial flow compressor rotor blade is cambered with an angle of attack over it and creates lift. This angle of attack is optimised to enhance the lift duty, and the rotor blades are attached to the compressor disc so that they can turn, accelerate the flow and increase the kinetic energy. It is necessary to add swirl (turning) to the air to be deflected at the required angle. A high deflection of the air will contribute in the case where weight reduction of the machine is required by promoting lower number of stages. High fluid deflection in the rotor blades is a criterion for high stage temperature rise which is desirable to minimise the number of stages for a given overall pressure ratio. The turbomachinery nature of axial flow compressors imply that energy is imparted to the air by the rotor blades, which increase the total pressure. So, the stagnation pressure is increased as the rotor imparts swirl to the air. Apart from blade functions, this section of this paper looks at flow separation dynamics and phenomena, effect on performance and causes, as well as previous works on axial compressor performance. It highlights the problem, specific objectives, and expected contribution to knowledge. By the design of axial flow compressors, they have diffusing passages, which enables some diffusion to occur in the rotor. As a result of the diffusion in the rotor passages, the air velocity relative to the rotor is decreased. Unlike the rotor blades, the stator blades are fixed to the housing of the compressor. The functions of the stator blades are that they decelerate, remove swirl, diffuse the flow and increase the static pressure. Stator blade is important to have proper pressure flow by changing the energy associated with the swirl into pressure (Srinivas et al., 2017).

Friction drag acts against flow separation at the boundary while the pressure drag associated with wake (pressure drag) increases with flow separation. Wake is turbulent in nature with eddies and mixing causing pressure losses. Moreover, compressor blade performance deteriorates at certain level of relative inlet Mach number that may trigger the relative Mach numbers within the blade passages to exceed unity, and more losses occur due to shock waves and thicker boundary layers. The axial flow compressor blade needs caution in the design to enable the production of an aerodynamically efficient as well as loss minimizing unit. Many variables are taken into account in the design process including air properties, blade pitch-chord ratio, and hub-tip ratio and diffusion concerns. Some other factors include the optimum engine speed, pressure ratio, air angles, blade angles, incidence angle, and off design conditions of operation. The choice is guided by seeking optimality, while not violating a number of performance, aerodynamic, structural and installation constraints (Kolias et al., 2021). Previously, blade failures have been traced to poor design that is why parameter values that meet performance requirement should be selected. Drastic improvement has been made in compressor blade profile design, hub to tip design and also tip to hub design (Srinivas et al., 2017).

Furthermore, the design should be such that gives allowance from calculations to enhance a wider range of operating conditions. Most common stall symptoms are fluctuations in pressure, rotor's rpm, exhaust gas temperature and air flow (Laskowski, 2017). Since the blade angle has to be fixed, it is proper to optimise its value to take care of changes in the air relative angle due to varying conditions. The air angles should allow good turning angle and air deflection in the rotor and stator. Diffusion occurs as the air flows through the blade passages. Small pressure increases is permitted in the stages, hence the increment in the cross sectional area of the diffusing flow passages should be moderate. It is important to ensure this because of the adverse pressure gradient against the flow. The most should be obtained from the diffusion process by ensuring minimum stagnation pressure losses. A previous research sought a simplified solution to determine the surge margin by experimenting with various three dimensional (3-D) computational fluid models; and from the research results by Muchowski and Gubernat (2021) a comparison between turbulence models and measurement proves that Shear Stress Transport (SST) turbulence model is not well distributed through the speed when compared with measurement data and Wilcox turbulence model. The concern for insight into surge behavior necessitated experimental analysis and surge modeling of a multistage compressor. From the results obtained in the study carried out by Munari et al. (2017), the actual data trend in surge condition differs from the model one only in terms of variation of mass flow rate, around the zero mass flow point. Generalised map can help detect choke region, and there is the need to keep a good choke margin to prevent failure of the blades.

In order to deal with convergence problem close to or within the choke region, an approach to model choking conditions at blade row and overall compressor level is proposed; choking is calculated in a transparent way, allowing the user to know any-time where along the flow path choking has occurred and what conditions caused it (Kolias et al., 2021). Other authors have viewed problem of flow distortion from transonic flows. The objective is to find numerical solutions to the unsteady and non uniform flow. According to Srinivas et al. (2018), the axial flow compressor distorted flow problem is modelled and analysed by means of a systematic three-dimensional numerical approach. Their results indicated that separation of the flow was high on the pressure side of the blade, with the distortion effect more pronounced near the tip region and as well as the hub corners of the blade. The model proved to satisfactorily be able to predict flow distortion at Mach numbers range of 0.8 to 1.2. Other reports have also shown how axial compressor performance can be evaluated using 1, 2 or 3-D methods with results from 1-D method showing good agreement with experimental data. A 1-D model was developed to predict design and off design performance of an axial flow compressor coupled to a turbine. Experimental data are obtained from tests of the axial compressor of a gas turbine engine in Sharif University gas turbine laboratory and consequently the running line is attained. As a result, the two important extremities of compressor performance including surge and choking conditions are obtained through 1-D and 3-D modelling (Peyvan and Benisi, 2016). The research results showed good agreement when the 1-D and 3-D models were compared with the experimental plant, and concluded that performance modelling can be sufficiently carried out using 1-D approach.

This work is novel for its directed concern on the GE (General Electric) Frame 9E compressor unit aerodynamic and performance characteristics. In essence, it used actual plant data to leverage innovation and improvement, and creates specific machine performance information advantage to be readily available to future researchers. The intention of this research is to provide performance and aerodynamic details on a more specific commercial axial flow compressor by investigating the GE Frame 9E compressor unit to promote future research, performance improvement, and flow stability. The aim of this research is axial flow compressor aerodynamic and performance

analysis; the specific objectives are to study design theories, observations, practice and commercial plant data on axial flow compressor performance; model the GE Frame 9E performance coefficients, flow behavior and degree of reaction across the compressor stages using a validated Simulink model; determine the influence of rotor inlet absolute air (flow) angle and engine speed on flow stability and degree of reaction, and how pitch-chord ratio affects flow stability. This study intends to investigate the performance, distribution of the diffusion factor and degree of reaction, and the effect of varying engine speed and rotor inlet flow angle on the aforementioned for a GE Frame 9E axial flow compressor, and bring them to the fore. Also, to enable performance improvement and flow stability of commercial gas turbines especially in Nigeria, and enhance future research. In the following sections, the methodology, results and discussion, conclusion, and recommendation will be considered.

2.0 Material and Methods

2.1 Equipment: A plant data validated GE Frame 9E unit, a 17 stage axial flow compressor model developed with Simulink was used to carry out the performance investigation.

2.2 Procedure: Based on the problem, the simulation methodology, considered design principles and practice for modeling axial flow compressors, as well as observations and relevant data collection. These were applied to Simulink blocks to model the compressor in stages and then assembled into a full unit. Data input of parameters which included stagnation inlet temperatures and pressures, mass flow rate of air, rotor inlet absolute air angle, number of stages, rotational speed and pitch-chord ratio were applied to the model; simulation of performance values was carried out. The Simulink model was validated using actual data from a commercial plant, a GE Frame 9E unit. Finally, results were organised using tables and analysed.

2.3 Theory: The governing principles are:

The compressor rotor blade speed, U and actual stage temperature rise, ΔT_{OS} can be evaluated from equations (1) and (2)

$$U = 2\pi r_{av} N_r / 60 \quad (1)$$

$$\Delta T_{OS} = \lambda U C_{ax} (\tan \beta_1 - \tan \beta_2) / C_{pa} \quad (2)$$

where β_1 = relative inlet angle into rotor, β_2 = relative outlet angle from rotor, C_{pa} = specific heat at constant pressure for air, λ = work done factor, r_{av} = average annulus radius, N_r = rotational speed, and C_{ax} = air axial velocity.

Both parameters can influence the compressor performance. Higher blade speed increases compression and influence the stage efficiency across the compressor, while higher overall pressure ratio is obtained with lower number of stages at higher stage temperature rise, but can lead to increased diffusion in the blades, and reduce efficiency.

The number of compressor stages, N_s and stagnation temperature at compressor exit, T_{Oe} are given in equations (3) and (4)

$$N_s = \Delta T_O / \Delta T_{OS} \quad (3)$$

$$T_{Oe} = T_{Oi} (r)^{(n-1)/n} \quad (4)$$

where,

$$T_{Oe} = \Delta T_O + T_{Oi}$$

ΔT_O = stagnation temperature rise across the compressor, T_{Oi} = stagnation temperature at compressor inlet, $r = p_{Oe}/p_{Oi}$ = pressure ratio, p_{Oi} = stagnation pressure at compressor inlet, p_{Oe} = stagnation pressure at compressor exit, and n = polytropic index.

The relative angle at rotor inlet can be obtained by inputting the blade speed, axial velocity and air absolute angle at rotor inlet in equation (5)

$$\tan\beta_1 + \tan\alpha_1 = U/C_{ax} \quad (5)$$

where α_1 = absolute air angle at rotor inlet.

According to Obanor et al. (2015), the relative angles at rotor inlet, rotor outlet, and absolute air angle at rotor outlet are given in equations (6), (7) and (8)

$$\beta_1 = \tan^{-1}(U - C_{t1})/C_{ax} \quad (6)$$

$$\beta_2 = \tan^{-1}(U - C_{t2})/C_{ax} \quad (7)$$

$$\alpha_2 = \tan^{-1}(C_{t2})/C_{ax} \quad (8)$$

where C_{t1} = tangential velocity at rotor inlet, C_{t2} = tangential velocity at rotor outlet.

The velocity diagrams on a common blade speed indicating reduced relative velocities, diffusion in the rotor blade and change in whirl are shown in Figure 1.

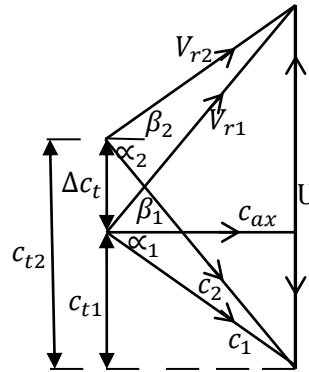


Figure 1: Relative Velocities Showing Rotor Diffusion

The diffusion occurring in the compressor stage leads to increased static pressure. To account for the extent of this static pressure increase due to diffusion in the rotor blades, a measure called the degree of reaction is defined. This non dimensional quantity has the potential for ordering the configuration of the velocity diagram based on the selected value. The amount of diffusion in the rotor and stator is controlled by the design of the compressor and it is often called the reaction of the stage (Avwunuketa et al., 2019). The angle between the inlet and outlet blade relative angles is known as the rotor fluid deflection and increased diffusion is induced as its value increases; de Haller number specifies a limit to the ratio of outlet to inlet relative velocities to control excessive diffusion. Diffusion factor is used to assign allowable diffusion index to blade regions, assess and evaluate flow stability; also high diffusion factors can induce higher stagnation pressure losses. Rotor fluid deflection, de Haller number, diffusion factor and degree of reaction are given in equations (9), (10), (11) and (12)

$$\delta = \beta_1 - \beta_2 \quad (9)$$

$$D_H = V_{r2}/V_{r1} \leq 0.72 \quad (10)$$

$$D_F = (1 - V_{r2}/V_{r1}) + (\Delta C_t/2V_{r1})(s/c) \quad (11)$$

$$R^\circ = C_{ax}(\tan \beta_1 + \tan \beta_2) / 2U \quad (12)$$

where ΔC_t = change in tangential velocity, s = blades pitch, c = chord length, and the ratio s/c is called the pitch-chord ratio, V_{r1} and V_{r2} are relative velocities at rotor inlet and outlet respectively.

A relation between mass flow and IGV angle according to Plis and Rusinowsky (2016) is presented in equation (13)

$$\dot{m}_{a1} = \dot{m}_{a1}^{\max} \cdot [1 - \text{VACF} \cdot (\text{IGV}^{\max} - \text{IGV})] \quad (13)$$

where \dot{m}_{a1} = compressed air flow depending on angle of IGV, \dot{m}_{a1}^{\max} = compressed air mass flow read from the generalised map of the compressor for the maximum IGVs angle (IGV^{\max}), VACF = variable angle correction factor, which determines the effect of variation in the angle of the IGVs on the compressed air mass flow.

The pressure rise, flow, stage efficiency, and temperature coefficients defined in equations (14), (15), (16), and (17) have been given for evaluating axial compressor stage performance,

$$p_{rc} = C_{pa} T_{OSi} (r_s^{(\gamma_a - 1)/\gamma_a} - 1) / U^2 \quad (14)$$

$$f_c = C_{ax1} / U \quad (15)$$

$$\eta_c = T_{OSi} (r_s^{(\gamma_a - 1)/\gamma_a} - 1) / \Delta T_{OS} \quad (16)$$

$$t_c = C_{pa} \Delta T_{OS} / U^2 \quad (17)$$

where r_s = stage pressure ratio, T_{OSi} = stagnation temperature at inlet of stage, C_{ax1} = axial velocity at inlet of stage, γ_a = ratio of specific heats for air, and [if $\Delta T_{OS} \ll T_{O1}$, $\eta_s = p_{rc}/t_c$]; T_{O1} being stage stagnation temperature at inlet to rotor. The assumptions made are shown in Table 1

Table 1: Assumptions

Compressor average inlet temperature, T_{O11} in Kelvin (K).	300.74
Compressor average exit temperature, T_{Oe2} (K).	631.8
Compressor average inlet pressure, p_{O11} (bar).	1.011
Mass flow rate of air, \dot{m}_a (kg/s), using air-fuel ratio in Eke et al. (2020) and commercial plant data.	397.8
Ratio of specific heats for air, γ_a (Saturday and Okumgba, 2020).	1.4
Specific heat at constant pressure for air gas, c_{pa} in kilojoule per kilogram per Kelvin (kJ/kgK) (Aderibigbe and Osunbor, 2019).	1.005
IGV angle range ($^\circ$).	33-84
Flow angle at the inlet to each stage, α_1 ($^\circ$).	15
Air axial velocity, C_{ax} in metres per second (m/s).	150
Average rotational speed, N_r in revolutions per second (rps),	50.41
Variable Angle Correction Factor (VACF) (Plis and Rusinowsky, 2016).	0.81
de Haller number .	0.72
Blade pitch to chord ratio, s/c .	0.5
Stage temperature rise (K).	19.47
Number of stages, N_s .	17

3.0 Results and Discussions

Table 2: Axial Flow Compressor Performance Values (50.41rps)

Stage	1	2	3	4	5	6	7	8	9	10	11	12	13	14	15	16	17
f_c	0.61	0.61	0.61	0.61	0.61	0.61	0.61	0.61	0.61	0.61	0.61	0.61	0.61	0.61	0.61	0.61	0.61
p_{rc}	0.30	0.30	0.30	0.30	0.30	0.30	0.30	0.30	0.30	0.30	0.30	0.30	0.30	0.30	0.30	0.30	0.30
t_c	0.33	0.33	0.33	0.33	0.33	0.33	0.33	0.33	0.33	0.33	0.33	0.33	0.33	0.33	0.33	0.33	0.33
η_c	0.92	0.92	0.92	0.92	0.92	0.92	0.92	0.92	0.92	0.92	0.92	0.92	0.92	0.92	0.92	0.92	0.92
α_2 (°)	39.11	43.09	43.37	43.66	43.96	44.28	44.60	44.96	45.32	45.69	46.08	46.49	46.91	47.36	47.83	48.32	47.13
β_1 (°)	53.67	51.31	51.37	51.42	51.49	51.55	51.62	51.67	51.74	51.80	51.87	51.93	52.01	52.07	52.14	52.22	53.67
β_2 (°)	39.17	34.70	34.34	33.95	33.55	33.12	32.68	32.17	31.66	31.10	30.51	29.86	29.18	28.44	27.64	26.78	28.84
δ (°)	14.49	16.61	17.03	17.47	17.93	18.42	18.94	19.50	20.08	20.70	21.36	22.07	22.82	23.63	24.50	25.44	24.83
D_F	0.36	0.37	0.37	0.37	0.37	0.37	0.38	0.38	0.38	0.38	0.39	0.39	0.39	0.39	0.40	0.40	0.40
R°	0.67	0.60	0.59	0.59	0.59	0.59	0.58	0.58	0.58	0.58	0.57	0.57	0.56	0.56	0.56	0.55	0.59

Table 3: Stage 17 Load and Performance Results (50.41rps)

r	\dot{m}_a	IGV(°)	U_{av}	r_{av}	f_c	p_{rc}	t_c	η_c	α_2 (°)	β_1 (°)	β_2 (°)	δ (°)	D_F	R°	ΔT_{Os} (K)
10.88	397.80	84.00	244.20	0.77	0.61	0.301	0.328	0.92	47.13	53.67	28.84	24.83	0.40	0.60	19.47
9.89	373.30	76.38	236.50	0.75	0.63	0.304	0.330	0.92	46.59	52.61	27.44	27.44	0.40	0.60	18.39
8.90	384.70	68.76	228.60	0.72	0.66	0.303	0.331	0.92	45.92	51.47	26.16	26.16	0.40	0.60	17.22
7.91	324.10	61.14	220.40	0.70	0.68	0.302	0.330	0.92	45.1	50.22	24.97	24.97	0.40	0.60	15.97
6.92	299.60	53.52	211.90	0.70	0.71	0.301	0.327	0.92	44.05	48.85	24.0	24.86	0.40	0.60	14.60
5.94	275.00	45.90	203.00	0.64	0.74	0.293	0.319	0.92	42.69	47.34	23.3	24.04	0.40	0.60	13.09
5.43	262.50	42.01	198.40	0.63	0.76	0.289	0.313	0.92	41.82	46.52	23.16	22.54	0.40	0.60	12.25

Table 4: Performance Values at Compressor Inlet of 288K (50rps)

Stage	1	17
f_c	0.63	0.63
p_{rc}	0.31	0.31
t_c	0.33	0.33
η_c	0.92	0.92
δ (°)	14.85	25.36
D_F	0.36	0.40
R°	0.66	0.58
ΔT_{os} (K)	18.65	18.65

Table 5: Performance Values at Different Rotational Speeds ($\Delta T_{os} = 19.47^\circ$, $r = 10.88$, Stage 17)

N_r (rps)	f_c	p_{rc}	t_c
40.00	0.77	0.48	0.52
50.41	0.61	0.30	0.33
60.00	0.52	0.21	0.23

Table 6: Rotational Speed and Degree of Reaction, Diffusion Factor at $\alpha_1 = 0$ ($\Delta T_{os} = 19.47^\circ$, $r = 10.88$, Stage 17)

N_r (rps)	R°	D_F	δ (°)
40.00	0.61	0.44	37.03
50.41	0.75	0.39	19.13
60.00	0.82	0.36	11.20

Table 7: Rotational Speed and Degree of Reaction, Diffusion Factor at $\alpha_1 = 10$ ($\Delta T_{os} = 19.47^\circ$, $r = 10.88$, Stage 17)

N_r (rps)	R°	D_F	δ (°)
40.00	0.47	0.45	42.65
50.41	0.64	0.39	22.72
60.00	0.73	0.36	13.18

Table 8: Rotational Speed and Degree of Reaction, Diffusion Factor at $\alpha_1 = 15$ ($\Delta T_{os} = 19.47^\circ$, $r = 10.88$, Stage 17)

N_r (rps)	R°	D_F	δ (°)
40.00	0.40	0.46	45.44
50.41	0.59	0.40	24.83
60.00	0.69	0.37	14.39

Table 9: Pitch-Chord Ratio and Diffusion Factor

$\Delta T_{os} = 19.47K$										
s/c	1.03	1.07	1.11	1.15	1.19	1.23	1.27	1.31	1.35	1.39
D_F	0.53	0.54	0.55	0.56	0.57	0.57	0.58	0.59	0.60	0.61
$\Delta T_{os} = 21K$										
s/c	0.30	0.40	0.50							
D_F	0.36	0.38	0.41							

The research results have been presented in tables above. Table 2 is axial flow compressor performance values, Table 3 is stage 17 load and performance results, Table 4 is performance values at compression inlet temperature of 288K and engine speed of 50rps, and Table 5 is performance values at different rotational speeds. More results are in Tables 6 to 8 which are rotational speed against degree of reaction and diffusion factor at rotor inlet air flow angles of 0° , 10° , and 15° respectively, and finally Table 9 is results of pitch-chord ratio and diffusion factor.

Performance parameters across the compressor stages indicated flow, temperature, pressure coefficients and efficiency of 0.61, 0.33, 0.3 and 0.92 respectively from the details provided in Table 2. This temperature coefficient which is not below 0.3 and not more than 0.4 is within limit, and keeping a good pressure rise coefficient to ensure satisfactory operation, with sufficient margin to prevent stall and choking conditions, since as temperature coefficient reduces flow coefficient increases. So a high efficiency is maintained across the compressor stages, which has the potential to promote overall plant performance. The values are not far from the limits of those that have been presented elsewhere. In a previous research, four compressors were designed with the same condition, the peak efficiency of the four stages was between 0.87 and 0.82, and the flow coefficient ranged from 0.48 to 0.62 (Wang et al., 2022).

The degree of reaction distribution was 0.67 and 0.59 at the first and last stage (stage 17) respectively, and it varied from 0.60 to 0.55 from the second to sixteenth stage, while the diffusion factor varied from 0.36 in the first stage to 0.4 in the last stage. Flow distortion is unlikely to occur considering the limit of the diffusion factor not surpassing 0.4 which is especially critical for the rotor tip region, thus ensuring lower blade loading and promoting reduced pressure losses. Moreover, diffusion through the blade passages was balanced progressively to the sixteenth stage which has the fairest sharing between rotor and stator blades. Some older literature have specified diffusion limit of 0.4 to 0.6, with up to 0.4 tolerated for rotor tip region, while for rotor hub and stator, a maximum of 0.6 is allowed, beyond which pressure losses are excessive. However, according to Xiang and Chen (2021) in general, the limit of diffusion factor is 0.55 to 0.6 for rotors and 0.6 to 0.75 for stators. Table 3 showed that for the last stage, flow coefficient increased to 0.76 as IGV angle and pressure ratio reduced while temperature coefficient was between 0.31 and 0.33 and pressure coefficients was about 0.3, and degree of reaction was 0.6.

The blade speed also decreased as IGV angle decreased at lower pressure ratios, and at the reduced speed of 198.4m/s, pressure ratio was 5.43 and the last stage temperature rise was 12.25K over the observed load range. The implication was that at lower blade speed the air was compressed below design value promoting lower pressure ratios and increased flow coefficient which tends to move the flow to choking. But stage isentropic efficiency was maintained, and flow instability was mitigated across the IGV load range as diffusion factor remained at 0.4, which underscores the influence of IGVs in controlling the amount of air mass flow to maintaining flow stability through the machine. In Table 4 when rotational speed and compressor inlet temperature were 50rps and 288K respectively for the design pressure ratio, the flow coefficient increased to 0.63 and pressure coefficient was up to 0.33, compared to 0.61 and 0.3 in Table 2. However, the diffusion factor was maintained at 0.4 while the degree of reaction reduced to 0.58. Increased pressure coefficient has the tendency to increase stage efficiency while reduced degree of reaction can enhance rotor and stator diffusion sharing.

Values of flow, temperature and pressure coefficients also reduced as rotational speed increased from the details in Table 5. At the reduced speed of 40rps the flow, temperature and pressure coefficients were found to be 0.77, 0.52 and 0.48 respectively, while at increased speed of 60rps the values were 0.52, 0.23 and 0.21 accordingly. Though the compressor maintained high stage efficiency, excessive deviation of engine speed from design value can shift the flow performance from acceptable limit. From the simulation results in Tables 6 to 8, the degree of reaction indicated higher values at lower rotor inlet absolute air angles, but the diffusion factor and rotor blade fluid deflection decreased. The various outputs showed increased degree of reaction, and decreased diffusion factor and rotor blade fluid deflection for the compressor stage as rotational speed was increased. Diffusion factor of 0.44 to 0.46 were observed at a speed of 40rps which was moving the flow more towards separation and higher losses at the rotor tip, while at a speed of 60rps, the diffusion factor was from 0.36 to 0.37.

A speed of 40rps according to the results would offer a degree of reaction from 0.4 to 0.61, and for a speed of 60rps, the value would be somewhere in the range of 0.69 to 0.82. A more balanced diffusion between the rotor and stator blades will be ensured at moderate flow angles and engine speed to maintain acceptable diffusion to reduce pressure losses in the rotor blades. The research also investigated the influence of pitch-chord ratio on the diffusion factor, and Table 9 shows that diffusion factor increased as the pitch-chord ratio increased. It revealed that at a pitch-chord ratio of 0.4 instead of 0.5 the diffusion factor can be limited to 0.38 even at a stage temperature rise of 21K which is above the design value of 19.47K (Table 7), thus further reducing the chances of flow separation. However, a pitch-chord ratio of 0.5 at this increased stage temperature rise increased the diffusion factor to 0.41. Pitch-chord ratio of 1.39 was found to induce a diffusion factor of 0.61 which can promote flow separation and excessive pressure losses even in the rotor hub and stator.

4.0 Conclusion

The aerodynamic and performance analysis of an axial compressor was studied. Investigation was centered on determining the performance details, distribution of diffusion factor, and degree of reaction of a GE Frame 9E compressor. Flow, temperature, pressure and efficiency coefficients of 0.61, 0.33, 0.3 and 0.92 respectively were observed across the compressor stages. The performance values were within limits of satisfactory operation, to prevent stall and choking conditions, and have the potential to promote overall plant performance. The degree of reaction distribution was between 0.67 and 0.59 at the first and last stage respectively, and it varied from 0.60 to 0.55 from the second to sixteenth stage, while the diffusion factor varied from 0.36 in the first stage to 0.4 in the last stage. Flow distortion is unlikely to occur, especially at the rotor tip region, thus ensuring lower blade loading and promoting reduced pressure losses. Diffusion through the blade passages was balanced progressively to the sixteenth stage which has the fairest sharing between rotor and stator blades.

Flow, temperature and pressure coefficients also reduced as rotational speed increased. At 40rps the flow, temperature and pressure coefficients were 0.77, 0.52 and 0.48 respectively, and at 60rps the values were 0.52, 0.23 and 0.21 accordingly. Though the compressor maintained high stage efficiency, excessive deviation of engine speed from design value can shift the flow performance from acceptable limit. The degree of reaction increased at lower rotor inlet absolute air angles, but decreased at lower engine speeds, while the diffusion factor decreased at lower rotor inlet absolute air angles, but increased at lower engine speeds. Diffusion factor of 0.44 to 0.46 was observed at 40rps which was moving the flow more towards separation and higher losses at the rotor tip. At 60rps, the diffusion factor was from 0.36 to 0.37. At 40rps, the degree of reaction was from 0.4 to 0.61, and at 60rps, a range from 0.69 to 0.82 was observed. A more balanced diffusion sharing between the rotor and stator blades will be ensured at moderate flow angles and engine speeds to maintain acceptable diffusion to reduce pressure losses in the rotor blades.

Diffusion factor increased as the pitch-chord ratio increased. At a pitch-chord ratio of 0.4, the diffusion factor can be limited to 0.38 even at a stage temperature rise of 21K which is above the design value of 19.47K, thus further reducing the chances of flow separation. A pitch-chord ratio of 0.5 at this increased stage temperature rise increased the diffusion factor to 0.41. Pitch-chord ratio of 1.39 was found to induce a diffusion factor of 0.61 which can promote flow separation and excessive pressure losses even in the rotor hub and stator. This study has made contribution to this field by bringing to the fore the performance details, the distribution of the diffusion factor and degree of reaction of a GE Frame 9E axial flow compressor, and the influence of engine speed and rotor inlet flow angle on them.

5.0 Recommendation

Moderate inlet flow angles should be allowed in the design of axial flow compressors to mitigate flow separation and instabilities. The rotor inlet flow angle and engine speed should be controlled to obtain a more balanced diffusion sharing between the rotor and stator blades. In the event of stage temperature rise above design, it should combine with a lower pitch-chord ratio to improve flow stability.

Nomenclature

C_1 = Inlet absolute velocity, m/s;
 C_2 = Outlet absolute velocity, m/s;
 C_{ax} = Axial velocity, m/s;
 C_{ax1} = Axial velocity at inlet of stage, m/s;
 C_{pa} = Specific heat at constant pressure for air, kJ/kgK;
 C_{t1} = Inlet tangential velocity, m/s;
 C_{t2} = Outlet tangential velocity, m/s;
 c = Chord length, m;
 D_F = Diffusion factor;
 D_H = de Haller number;
 f_c = Flow coefficient;
 \dot{m}_{a1} = Inlet mass flow rate of air, kg/s;
 \dot{m}_{a1}^{max} = Inlet maximum mass flow rate of air, kg/s;
 n = Polytropic index;
 N_r = Rotational speed, rps;

N_s = Number of stages;
 p_{0e} = Stagnation pressure at compressor exit, bar;
 p_{0i} = Stagnation pressure at compressor inlet, bar;
 p_{0i1} = Stagnation pressure at compressor inlet at point 1, bar;
 p_{rc} = Pressure coefficient;
 R^o = Degree of reaction;
 r = Pressure ratio;
 r_{av} = Annulus average radius, m;
 r_s = Stage pressure ratio;
 s = Blade pitch, m;
 T_{01} = Stage stagnation temperature at inlet to rotor, K;
 T_{0e} = Stagnation temperature at compressor exit, K;
 T_{0e2} = Stagnation temperature at compressor exit at point 2, K;
 T_{0i} = Stagnation temperature at compressor inlet, K;
 T_{0i1} = Stagnation temperature at compressor inlet at point 1, K;
 T_{0Si} = Stage stagnation inlet temperature, K;
 t_c = Temperature coefficient;
 U = Blade speed, m/s;
 V_{r1} = Inlet relative velocity, m/s;
 V_{r2} = Outlet relative velocity, m/s;
 α_1 = Inlet absolute air angle, ($^\circ$);
 α_2 = Outlet absolute air angle, ($^\circ$);
 β_1 = Inlet relative air angle, ($^\circ$);
 β_2 = Outlet relative air angle, ($^\circ$);
 γ_a = Ratio of specific heats for air;
 ΔC_t = Change in tangential velocity, m/s;
 ΔT_o = Stagnation temperature rise across the compressor, K;
 ΔT_{oS} = Stage stagnation temperature rise, K;
 δ = Rotor blade fluid deflection, ($^\circ$);
 η_c = Efficiency coefficient;
 η_s = Stage efficiency,
 λ = Work-done factor
 1-D = One Dimensional;
 2-D = Two Dimensional;
 3-D = Three Dimensional;
 GE = General Electric;
 IGV = Inlet Guide Vane;
 IGV^{max} = Maximum Inlet Guide Vane Angle;
 SST = Shear Stress Transport;
 VACF = Variable Angle Correction Factor.

References

- Aderibigbe, D.A., and Osunbor, G., 2019. Performance of a 270 MW Gas power plant using exergy and heat rate. *Energy and Power Engineering (EPE)*, 11, 15-34. <https://doi.org/10.4236/epe.2019.112002>
- Avwunuketa, A., Ajao, T.A. and Adamu, M.L., 2019. Performance evaluation of Axial flow compressor using stages characteristics. *SSRG International Journal Journal of Thermal Engineering (SSRG-IJTE)*, 5(2), 1-7. [doi:10.14445/23950250/ijte-v5i2p101](https://doi.org/10.14445/23950250/ijte-v5i2p101)
- Eke, M.N., Okoroigwe, E.C., Umeh, S.I. and Okonkwo, P., 2020. Performance improvement of a Gas turbine power plant in Nigeria by exergy analysis: A Case of Geregu I. *Open Access Library Journal*, 7: e6617. <https://doi.org/10.4236/oalib.1106617>

- Kolias, I., Alexiou, A., Aretakis, N., and Mathiodakis, K., 2021. Axial compressor Mean-line analysis: choking modelling and fully-coupled integration in engine performance simulations. *International Journal of Turbomachinery Propulsion and Power*, 6(4), 1-23. doi.org/10.3390/ijtpp610004
- Laskowski, P., 2017. Factors influencing Axial compressor stalls. *Scientific Journal of Silesian University of Technology. Series Transport*, 95, 90-96. <https://doi.org/10.20858/sjsutst.2017.95.9>
- Muchowski, R. and Gubernat, S., 2021. Influence of Axial compressor model simplification and Mesh density on Surge Margin evaluation. *Advances in Science and Technology Research Journal*, 15(3), 243-253. <https://doi.org/10.12913/22998624/140541>
- Munari, E., Morini, M. and Pinelli, M., 2017. Experimental investigation and modelling of surge in a multistage compressor. *Energy Procedia*, 105, 1751-1756. <https://doi.org/10.1016/j.egypro.2017.03.503>
- Obanor, A.I., Unuareokpa, O.J. and Egware, H.O., 2015. An algorithm for the design of an Axial flow compressor of a Power Generation Gas Turbine. *Nigerian Journal of Technology (NIJOTECH)*, 34(2), 314-324. <http://dx.doi.org/10.4314/nit.v34i2.16>
- Peyvan, A. and Benisi, A.H., 2016. Axial flow compressor performance prediction in design and off design conditions through 1-D and 3-D modeling and experimental study. *Journal of Applied Fluid Mechanics (JAFM)*, 9(5), 2149-2160. [doi:10.18869/acadpub.jafm.68.236.25222](https://doi.org/10.18869/acadpub.jafm.68.236.25222)
- Plis, M. and Rusinowsky, H., 2016. Mathematical modeling of an Axial compressor in a Gas Turbine Cycle. *Journal of Power Technologies*, 96(3), 194-199. <https://papers.its.pw.edu.pl/index.php/article/view/951>
- Saturday, E.G. and Okumgba, T.J., 2020. Performance assessment of gas turbine power plants. *Saudi Journal of Engineering and Technology (Saudi J Eng Technol)*, 5(6), 265-270. [doi:10.36348/sjet.2020.v0i06.002](https://doi.org/10.36348/sjet.2020.v0i06.002)
- Srinivas, G. Raghunandana, K. and Shenoy, B.S., 2017. Recent developments of Axial flow compressors under transonic flow conditions. *IOP Conference Series: Materials Science and Engineering*, 197 012078, 1-10. [doi:10.1088/1757-899X/197/1/012078](https://doi.org/10.1088/1757-899X/197/1/012078)
- Srinivas, G. Raghunandana, K., and Shenoy, B.S., 2018. Axial-flow compressor analysis under distorted phenomena at transonic flow conditions. *Cogent Engineering*, 5(1), 1526458. <https://doi.org/10.1080/23311916.2018.1526458>
- Wang, R., Yu, X., Liu, B. and An, G., 2022. Effects of loading level on the variation of flow losses in subsonic Axial compressors. *Energies* 2022, 15(17), 6251. <https://doi.org/10.3390/en15176251>
- Xiang, H. and Chen, J., 2021. Aerothermodynamics Optical design of a multistage Axial compressor in a Gas Turbine using directly manipulated free-form deformation. *Case Studies in Thermal Engineering*, 26, August 2021, 101142.